



# Piperlongumine induces pancreatic cancer cell death by enhancing reactive oxygen species and DNA damage

Harsharan Dhillon\*, Shireen Chikara, Katie M. Reindl

*Department of Biological Sciences, North Dakota State University, Fargo, ND 58105, USA*



## ARTICLE INFO

### Article history:

Received 8 April 2014

Received in revised form 15 May 2014

Accepted 16 May 2014

Available online 11 June 2014

### Keywords:

ROS

Pancreatic cancer

Natural products

## ABSTRACT

Pancreatic cancer is one of the most deadly cancers with a nearly 95% mortality rate. The poor response of pancreatic cancer to currently available therapies and the extremely low survival rate of pancreatic cancer patients point to a critical need for alternative therapeutic strategies. The use of reactive oxygen species (ROS)-inducing agents has emerged as an innovative and effective strategy to treat various cancers. In this study, we investigated the potential of a known ROS inducer, piperlongumine (PPLGM), a bioactive agent found in long peppers, to induce pancreatic cancer cell death in cell culture and animal models. We found that PPLGM inhibited the growth of pancreatic cancer cell cultures by elevating ROS levels and causing DNA damage. PPLGM-induced DNA damage and pancreatic cancer cell death was reversed by treating the cells with an exogenous antioxidant. Similar to the *in vitro* studies, PPLGM caused a reduction in tumor growth in a xenograft mouse model of human pancreatic cancer. Tumors from the PPLGM-treated animals showed decreased Ki-67 and increased 8-OHdG expression, suggesting PPLGM inhibited tumor cell proliferation and enhanced oxidative stress. Taken together, our results show that PPLGM is an effective inhibitor for *in vitro* and *in vivo* growth of pancreatic cancer cells, and that it works through a ROS-mediated DNA damage pathway. These findings suggest that PPLGM has the potential to be used for treatment of pancreatic cancer.

© 2014 The Authors. Published by Elsevier Ireland Ltd. This is an open access article under the CC BY-NC-ND license (<http://creativecommons.org/licenses/by-nc-nd/3.0/>).

## 1. Introduction

Pancreatic cancer is one of the most deadly cancers in the United States with a 5-year survival rate of less than 6% [1]. The vast majority of pancreatic cancer patients present with advanced disease, at which point surgery is no longer

an option [2]. The best chemotherapy currently available has a minimal impact on advanced pancreatic cancers, and extends patients' lives by only a couple of months [3]. There is a critical need to develop new therapeutic strategies to enhance the survival of pancreatic cancer patients.

A new approach for pancreatic cancer treatment is the use of reactive oxygen species (ROS)-inducing small molecules that take advantage of the altered redox state in cancer cells [4–6]. Cancer cells exhibit elevated levels of ROS as well as antioxidant enzymes [7]. As a result, cancer cells are more vulnerable than normal cells to agents that induce further oxidative stress or impair the antioxidant response [8].

Several ROS-inducing small molecules have been tested in clinical trials for the treatment of pancreatic cancer. The ROS inducer β-lapachone causes cytotoxicity in

**Abbreviations:** 8-OHdG, 8-hydroxy-2'-deoxyguanosine; DCFDA, 2,7-dichlorodihydrofluorescein diacetate; DMSO, dimethyl sulfoxide; GSTP1, glutathione S-transferase P1; HO1, heme oxygenase 1; NAC, N-acetyl cysteine; PPLGM, piperlongumine; pChk1, phospho checkpoint kinase 1; ROS, reactive oxygen species; SOD1, superoxide dismutase 1.

\* Corresponding author at: Department of Biological Sciences, North Dakota State University, 1340 Bolley Drive, Stevens Hall 201, Fargo, ND 58105, USA. Tel.: +1 701 231 9427; fax: +1 701 231 7149.

E-mail address: [harsharan.randhawa@my.ndsu.edu](mailto:harsharan.randhawa@my.ndsu.edu) (H. Dhillon).

NAD(P)H:quinone oxidoreductase (NQO1)-overexpressing pancreatic tumors by modulating PARP, NAD<sup>+</sup>/ATP levels, leading to single-stranded DNA breaks, and necrosis [9,10]. Clinical trials of β-lapachone in combination with gemcitabine have been used for the treatment of metastatic pancreatic adenocarcinoma. Further, phase I and II clinical studies for imexon, a small molecule pro-oxidant have been conducted in pancreatic cancer patients [11]. Imexon induces apoptosis in pancreatic cancer cells by elevating ROS levels and causing cell cycle arrest [12].

Given the promise of ROS-inducing agents for cancer treatment, we investigated the effects of the ROS-inducer piperlongumine (PPLGM) on pancreatic cancer cell death *in vitro* and *in vivo*. PPLGM is an alkaloid found in the fruits of long pepper plants that displays potent growth-inhibitory properties in a variety of cancer cell lines and various animal models. Interestingly, PPLGM has been shown to be non-toxic to several normal cell types and tissues [13,14]. In this study, PPLGM's effect on ROS levels, DNA damage, and cell death were evaluated in cell culture and animal models to evaluate the potential of PPLGM as an alternative therapeutic approach to treating pancreatic cancer.

## 2. Materials and methods

### 2.1. Materials

Piperlongumine (PPLGM) was purchased from Indofine Chemical Company (Catalog#: P-004, 97%, Hillsborough, NJ). PPLGM was dissolved in 100% DMSO at a stock concentration of 10 mM and then diluted in water to a working concentration. The final concentration of PPLGM was in the range of 0.1–20 μM. pChk1 (S296) and total Chk1 antibodies were purchased from Cell Signaling Technologies (Danvers, MA). Mouse anti Ki-67 primary antibody (clone MM1) was purchased from Vector Labs (Burlingame, CA). Anti-8-hydroxy-2' deoxyguanosine (8-OHdG) monoclonal (N45.1) primary antibody was purchased from Japan Institute for the Control of Aging (JalCa, Shizuoka, Japan). CF633-conjugated goat anti-mouse IgG secondary antibody was purchased from VWR (Atlanta, GA).

### 2.2. Cell culture

The PANC-1 and MIA PaCa-2 cell lines were obtained from ATCC in 2013 (Manassas, VA) and cultured at 37 °C with 5% carbon dioxide in Dulbecco's Modified Eagle's (Thermo Scientific, Waltham, MA) medium supplemented with 10% fetal bovine serum (Atlanta Biologicals, Lawrenceville, GA). The BxPC-3 cell line was also obtained from ATCC and cultured in RPMI-1640 (Thermo Scientific, Waltham, MA) medium supplemented with 10% fetal bovine serum. The cell lines were subcultured by enzymatic digestion with 0.25% trypsin/1 mM EDTA solution (Thermo Fisher) when they reached approximately 70% confluency.

### 2.3. AlamarBlue® cell toxicity assay

PANC-1, MIA PaCa-2, and BxPC-3 cells ( $5.0 \times 10^3$ ) were seeded into individual wells of a 96-well plate, and 24 h

later were treated with PPLGM (0–20 μM) after which alamarBlue® (AbD Serotech, Raleigh, NC) was added at a final concentration of 10% and incubated at 37 °C for 4 h. The oxidized form of the dye is converted into the reduced form by a mitochondrial enzyme present in the viable cells. Absorbance was measured at 570 and 600 nm on a plate reader. The cells were monitored daily over a 3-day period to gauge potential shifts in absorbance. The percent reduction in alamarBlue® over time for each treatment was calculated by using the following formula:

$$\begin{aligned} \text{\% reduction in alamarBlue}^{\circledR} \\ = \frac{117,216(A_1) - 80,586(A_2)}{155,677(B_1) - 14,652(B_2)} \times 100 \end{aligned}$$

In the formula, 117,216 and 80,586 are constants representing the molar extinction coefficients of alamarBlue® at 570 and 600 nm, respectively, in the oxidized form; whereas 115,677 and 14,652 are constants representing the molar extinction coefficients of alamarBlue® at 570 and 600 nm, respectively, in the reduced form.  $A_1$  and  $A_2$  represent absorbance of wells treated with PPLGM at 570 and 600 nm, respectively.  $B_1$  and  $B_2$  represent absorbance of untreated wells at 570 and 600 nm, respectively. A reduction in alamarBlue® absorbance correlates to a decrease in cell viability. The data represent the % cell viability relative to control ± standard deviation in eight replication wells per treatment for three independent experiments. The half maximal inhibitory concentrations ( $IC_{50}$ ) were calculated by fitting the dose-response curves derived after plotting the percent cell viability against the log concentration. Eight replicate wells were used per treatment and the experiments were performed in triplicate for each cell line.

### 2.4. Clonogenic-survival assay

The clonogenic-survival assay tests the long term survival ability of cells in the presence of an anticancer agent. PANC-1, MIA PaCa-2, and BxPC-3 cells ( $5 \times 10^2$ ) were seeded into individual wells of a 24-well plate. The next day, the cells were treated with 0–20 μM PPLGM for 24 h. The cells were allowed to grow and form colonies for 14 days. After 14 days, the colonies were fixed in a solution of methanol and acetic acid (3:1), stained with 0.5% crystal violet, and counted manually. Four replicate experiments were performed for each cell line.

### 2.5. Measurement of ROS by the 2,7-dichlorodihydrofluorescein diacetate (DCF-DA) assay

Approximately  $5.0 \times 10^5$  cells/ml of all three pancreatic cancer cell lines were suspended in culture medium and treated with 10 μM PPLGM for 6 h. After treatment, cells were harvested by centrifugation and re-suspended in 10 μM DCF-DA (Life Technologies, Carlsbad, CA) in PBS. The cells were incubated at 37 °C for 30 min before flow cytometric analysis using an Accuri C6 Flow Cytometer. The experiments were performed in triplicate for each cell line.

## 2.6. Q-PCR

Total RNA was isolated from PANC-1 cells ( $1.0 \times 10^6$  cells) using the Fisher SurePrep Kit (Waltham, MA) as per the manufacturer's instructions. 100 ng of total RNA were reverse transcribed into cDNA using the qScript cDNA synthesis kit (Quanta Biosciences, Gaithersburg, MD). Primers against human SOD1, GSTP1, and HO1 were designed using Primer Express software (version 2.0, Applied Biosystems), and synthesized by Integrated DNA Technologies (Coralville, IA). Primer sequences were as follows, HO-1 forward: AATTCTCTGGCTG-GCTTCCT; HO-1 reverse: CATAGGCTCCTCCCTCCTTCC; GSTP1 forward: CAGGAGGGCTCACTCAAAGC; GSTP1 reverse: AGGTGACGCAGGATGGTATTG; SOD1 forward: GCCTGCATGGATTCCATGTT, SOD1 reverse: TGGCCCAC-CGTTTTCT. Steady-state mRNA levels of antioxidant genes were determined for the cDNAs by real-time PCR using PerfeCTa SYBR Green FastMix (Quanta Biosciences). The cycling parameters were 95 °C for 10 min followed by 40 cycles of 95 °C for 30 s and 60 °C for 1 min and a dissociation program that included 95 °C for 1 min, 55 °C for 30 s and 95 °C for 30 s ramping up at 0.2 °C/s. One distinct peak was observed for the primer sets. The fold change in mRNA expression was calculated by comparing the 18S rRNA-normalized threshold cycle numbers ( $C_T$ ) in the PPLGM-treated cancer cells compared to the DMSO-treated cancer cells. Duplicate wells were run for each experiment and the experiments were performed in triplicate.

## 2.7. Cell survival assay

For determining cell survival, human pancreatic cancer cell lines ( $4.0 \times 10^5$  cells) were treated with the vehicle control (0.1% DMSO), 10 μM PPLGM, 3 mM N-acetyl cysteine (NAC), and 10 μM PPLGM in combination with 3 mM NAC for 24 h. The next day, images were taken using a Leica DMIL inverted microscope with a DFC290 digital color camera. The effect of treatments on the number of surviving pancreatic cancer cells can be viewed in the images.

## 2.8. DNA fragmentation assay

MIA PaCa-2 cells ( $5.0 \times 10^5$  cells) were seeded into individual wells of a 6-well plate, and 24 h later were treated with vehicle control (0.1% DMSO), 10 μM PPLGM, 3 mM N-acetyl cysteine (NAC), and 10 μM PPLGM in combination with 3 mM NAC for 24 h. After 24 h, the cells were washed twice with PBS, and the DNA was extracted using DNAzol reagent (Molecular Research, Cincinnati, OH, USA). Isolated DNA was resolved on 1.5% agarose gels containing ethidium bromide (EtBr) and images were captured using the Multilimage™ Light Cabinet (Alpha Innotech, San Leandro, CA). The experiments were performed in triplicate.

## 2.9. Western blot

MIA PaCa-2 cells ( $1 \times 10^6$  cells) were treated with or without 10 μM PPLGM and 5 μM GEM for 24 h. Cell pellets were lysed using an SDS lysis buffer (Cell Signaling

Technologies) containing protease and phosphatase inhibitors (Roche, Indianapolis, IN). Samples were briefly sonicated to dissociate cell membranes. Sixty micrograms of total protein isolated from PPLGM or GEM-treated MIA PaCa-2 cells were separated on 10% SDS-polyacrylamide gels at 100 V for 1 h. Proteins were transferred to nitrocellulose membranes at 100 V for 70 min at 4 °C. Blots were then probed overnight at 4 °C with primary antibodies. The next day, blots were rinsed with 1 × TBS-tween (0.1%) and probed with secondary antibody for 1 h at room temperature. The western blots were analyzed using SuperSignal West Pico Chemiluminescent Substrate (Thermo Fisher Scientific, Rockford, IL) and images were captured using the MultiImage™ Light Cabinet (Alpha Innotech, San Leandro, CA). pChk1 (S296) levels were normalized to total Chk1 expression. Immunoblots were performed in triplicate and the image in the figure represents one typical replicate.

## 2.10. Nude mouse studies

Six- to 8-week old female athymic nude mice (Nu/Nu) were purchased from Charles River Laboratories (Wilmington, MA). The mice were maintained in sterile conditions using the Innovive IVC System (Innovive, San Diego, CA), following the protocol approved by North Dakota State University's Institutional Animal Care and Use Committee (IACUC). The mice were acclimated for 1 week before experimental manipulation. Tumor xenografts were established by subcutaneous injection of  $2.0 \times 10^6$  PANC-1 cancer cells in 0.1 ml PBS in the rear flank of the animals. Once tumor masses became established, the mice were randomly divided into two groups ( $n=8$ ). Group 1 served as the control group and received dimethyl sulfoxide (DMSO, 1%) by intraperitoneal injection. Group 2 received 2.4 mg PPLGM/kg body weight daily for 30 days by intraperitoneal injection. PPLGM was dissolved initially in DMSO and further diluted in PBS before administering to the mice, and the final concentration of DMSO was 1%. Two axes of the tumor (L, longitudinal axis; W, shortest axis) were measured with a caliper three times a week and each mouse was weighed weekly. The tumor volume was calculated as:  $V = (L \times W^2)/2$ . Following four weeks of experimental treatment, the animals were euthanized in an isoflurane chamber followed by cervical dislocation.

## 2.11. Immunohistochemistry

Tumor tissues from control and PPLGM-treated mice were collected and fixed for 24 h in formaldehyde. Paraffin-embedded 5 μm thick sections of tumor tissues were prepared. Sections were deparaffinized with histoclear and ethanol, followed by antigen retrieval in 10 mM sodium citrate buffer (0.05% Tween 20, pH 6.0) using an autoclave method. The sections were blocked for 20 min in blocking buffer (10% normal goat serum in TBST) and incubated with primary antibodies (Ki-67 [1:100] and 8-OHDG [1:20]) overnight at 4 °C. The next day, sections were incubated with CF633-conjugated goat anti-mouse secondary antibody (1:250) for an hour at room temperature,

and were visualized using a Zeiss inverted Axio Observer Z1 microscope after mounting a coverslip using Hard-set Mounting media with DAPI (Vector Labs, Burlingame, CA).

## 2.12. Statistical analyses

Data are presented as means  $\pm$  standard deviation for at least 3 independent experiments. The significance of differences between groups was determined using a Student's *t*-test with statistical significance defined as  $p < 0.05$ . Statistical analyses were performed using SigmaPlot v12.

## 3. Results

### 3.1. PPLGM causes concentration- and time-dependent growth inhibition of pancreatic cancer cells

The short-term, growth inhibitory effects of PPLGM on three pancreatic cancer cell lines were investigated using the alamarBlue® assay. The cell lines were treated with either the vehicle control (DMSO, <0.1%) or increasing concentrations of PPLGM (0.1–20  $\mu$ M) for 0–3 days, and cell growth was assessed each day. PPLGM induced a concentration and time-dependent decrease in the viability of PANC-1, MIA PaCa-2, and BxPC-3, with IC<sub>50</sub> values of 4.2, 4.6, and 4.2  $\mu$ M, respectively, at 72 h (Fig. 1A–C). Twenty

micromolar PPLGM significantly inhibited the growth of all pancreatic cancer cell lines by day 1, while 5  $\mu$ M PPLGM significantly inhibited growth by day 2. BxPC-3 cells were slightly more sensitive to lower concentrations of PPLGM than PANC-1 and MIA PaCa-2 cells, where the 2.5  $\mu$ M and 1  $\mu$ M treatments significantly reduced BxPC-3 growth at days 2 and 3, respectively.

### 3.2. PPLGM causes a concentration-dependent decrease in long-term survival of pancreatic cancer cells

To evaluate the effects of PPLGM on long-term survival of pancreatic cancer cell lines, a clonogenic survival assay was performed. PANC-1, MIA PaCa-2, and BxPC-3 cells were seeded at a low density in culture dishes, allowed to adhere overnight, treated with either the vehicle control (DMSO) or increasing concentrations of PPLGM (0.1–10  $\mu$ M), and then incubated, undisturbed, for 14 days. The total number of colonies formed was counted for each culture dish. The data represent the average number of colonies formed for three replicates of the respective treatment groups. The results show that PPLGM caused a concentration-dependent decrease in the number of colonies formed for all three cell lines as compared to the controls (Fig. 1D). MIA PaCa-2 and BxPC-3 cells were particularly sensitive to PPLGM, and no cells survived for the 5 and 10  $\mu$ M treatments.

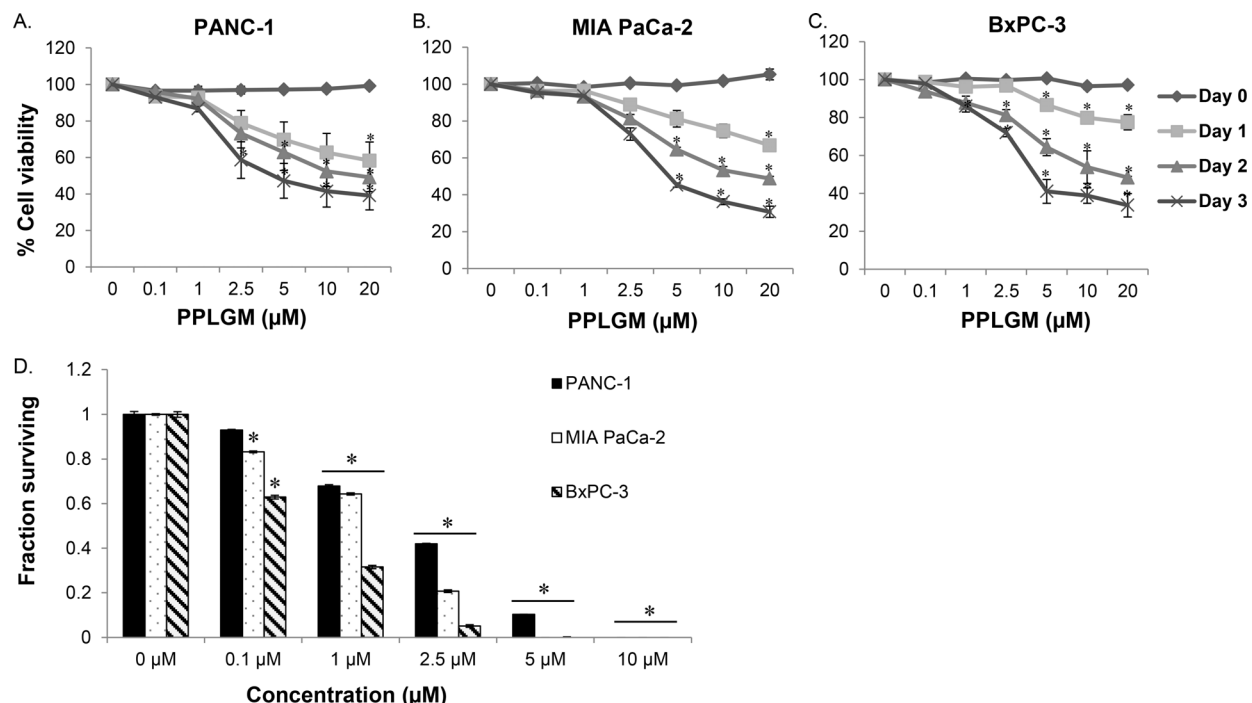


**Fig. 1.** Effect of PPLGM on the growth of three pancreatic cancer cell lines. The three pancreatic cancer cell lines (A) PANC-1, (B) MIA PaCa-2, and (C) BxPC-3 were treated with various concentrations (0–20  $\mu$ M) of PPLGM for up to 3 days. The short-term growth of pancreatic cancer cells was measured spectrophotometrically using an alamarBlue® assay at days 0, 1, 2, and 3. The metabolic activity of living cells is detected by a change in color of alamarBlue® from an oxidized (blue) form to a reduced (purple) form. The data represent the average percent cell viability relative to control  $\pm$  standard deviation in eight replicate wells per treatment for three independent experiments. Statistical significance was determined by Student's *t*-test ( $p < 0.05$  for PPLGM-treated vs. vehicle control). (D) The long-term growth of all three cell lines was determined by calculating the fraction of cells surviving in the presence of PPLGM (0–10  $\mu$ M) over the course of 14 days by clonogenic survival assay. The data represent the average  $\pm$  standard deviation for three independent experiments for PANC-1, MIA PaCa-2, and BxPC-3 cells. Statistical significance was determined by Student's *t*-test ( $p < 0.05$  for PPLGM-treated vs. vehicle control).

### 3.3. PPLGM elevates ROS levels in pancreatic cancer cell lines without significantly altering the expression of antioxidant response enzymes

PPLGM is known to cause elevated levels of ROS in cancer cell lines [13], and enhanced ROS levels are associated with cancer cell death for various agents [15]. Therefore, we examined the role of ROS in PPLGM-induced pancreatic cancer cell death. PANC-1, MIA PaCa-2, and BxPC-3 cells were treated with 10  $\mu$ M PPLGM for 6 h followed by staining for 30 min with the redox-sensitive fluorescent probe DCFDA. Intracellular ROS oxidize DCFDA to the highly fluorescent DCF compound which can be detected by flow cytometry. Fig. 2A shows PPLGM increases the production of ROS in all three pancreatic cancer cell lines compared to the vehicle control treatment. The PPLGM-induced ROS levels were quantified and the results show that the MIA PaCa-2 cell line experienced a 24-fold increase in ROS relative to the control-treated cells, followed by PANC-1 cells with a 9-fold increase, and Bx-PC3 cells with an 8-fold increase (Fig. 2B).

ROS levels can increase within a cell by two primary mechanisms: (1) increased ROS production or (2) decreased antioxidant scavenging. To determine if PPLGM elevates ROS by inhibiting the antioxidant capacity of pancreatic cancer cells, we performed qPCR to measure the mRNA transcript levels of SOD1, GSTP1, and HO1. The mRNA levels for these antioxidant enzymes were slightly, but not significantly ( $p > 0.05$ ) elevated in PPLGM-treated pancreatic cancer cells (Fig. 2C).

### 3.4. An exogenous antioxidant partially blocks PPLGM-induced pancreatic cancer cell death

We next evaluated the ability of an exogenous antioxidant to reverse the effects of PPLGM for pancreatic cancer cell death. The three pancreatic cancer cell lines were treated for 24 h with 3 mM N-acetyl cysteine (NAC) alone and in combination with PPLGM. Images of the culture dishes reveal that PPLGM reduced the number of surviving pancreatic cancer cells and that NAC could partially block this effect (Fig. 2D).

### 3.5. PPLGM induces DNA damage which is blocked by the antioxidant NAC

Increased ROS levels are known to cause DNA damage. Therefore, a DNA laddering assay was done to investigate the potential involvement of PPLGM-induced ROS in causing DNA damage resulting in pancreatic cancer cell death. MIA PaCa-2 cells were treated with, DMSO (0.1%), 10  $\mu$ M PPLGM, or gemcitabine (GEM) as a positive control for 24 h. DNA was isolated from the cells and loaded onto an agarose gel. Increased DNA laddering was observed in PPLGM-treated cells compared to the control cells (Fig. 3A and B) indicating that PPLGM causes DNA damage for pancreatic cancer cells. Further evidence of DNA damage was shown by enhanced pChk1 (S296) protein expression in PPLGM-treated cells as compared to the control cells (Fig. 3C and D). Cells that were treated with the antioxidant NAC + PPLGM

**Table 1**  
Effect of PPLGM on tumor, organ, and final weight of mice.

	Control	PPLGM
Tumor (mg)	55.9 ± 19.1	27.7 ± 4.7
Kidney (mg)	354.3 ± 13.9	330.8 ± 11.6
Liver (mg)	1105.9 ± 24.1	1088.4 ± 58.0
Lung (mg)	172.6 ± 8.8	169.5 ± 5.3
Spleen (mg)	102.4 ± 12.8	103.7 ± 7.2
Final weight (g)	21.8 ± 1.1	21.7 ± 0.6

showed reduced DNA damage compared to those treated with PPLGM alone (Fig. 3E and F).

### 3.6. PPLGM suppresses the growth of tumor in a mouse xenograft model

Given the promising response of pancreatic cancer cell lines to PPLGM, we chose to further investigate the anti-cancer effects of PPLGM in an animal model of pancreatic cancer. PANC-1 human pancreatic cancer cells were injected subcutaneously into athymic nude mice. Tumor growth was significantly suppressed in mice treated with 2.4 mg PPLGM/kg (daily for 30 days) as compared to those treated with DMSO (1%) vehicle (Fig. 4). PPLGM-treated animals had, on average, tumors that were 50% the mass of tumors from control-treated animals (Table 1). The PPLGM treatment was well-tolerated and no significant changes were detected in overall animal mass or organ mass, as shown in Table 1.

### 3.7. PPLGM decreases proliferation and increases DNA damage in pancreatic tumors

Ki-67 cell proliferation and 8-hydroxy-2'-deoxyguanosine (8-OHDG) oxidative DNA damage markers were examined by immunohistochemical staining for PPLGM-treated and vehicle-treated tumors harvested from the mice. The tumors obtained from the PPLGM-treated mice exhibited notably less Ki-67-positive cells compared with tumors from the control mice (Fig. 5). Furthermore, tumors from PPLGM-treated mice showed markedly higher 8-OHDG levels compared with tumors from control mice (Fig. 5).

## 4. Discussion

ROS-inducing agents are an attractive alternative approach for treating pancreatic cancer [5,16,17]. The ROS-inducing agents  $\beta$ -lapachone and imexon induce apoptosis and necrosis in pancreatic cancer cells, and have been investigated in clinical trials for the treatment of pancreatic cancers [9–11]. Therefore, we investigated the potential of the small-molecule ROS inducer, PPLGM, for pancreatic cancer cell death. PPLGM is known to cause cancer-selective cell death through a ROS-dependent mechanism [13]. Here we show that PPLGM is toxic to PANC-1, MIA PaCa-2, and BxPC-3 pancreatic cancer cells. The cytotoxic effects of PPLGM have previously been shown in PANC-1 and MIA PaCa-2 cells [13]. Both of these cell lines are *K-ras* mutant whereas BxPC-3 cells contain wild-type *K-ras*. Our data supports previous results and extends the

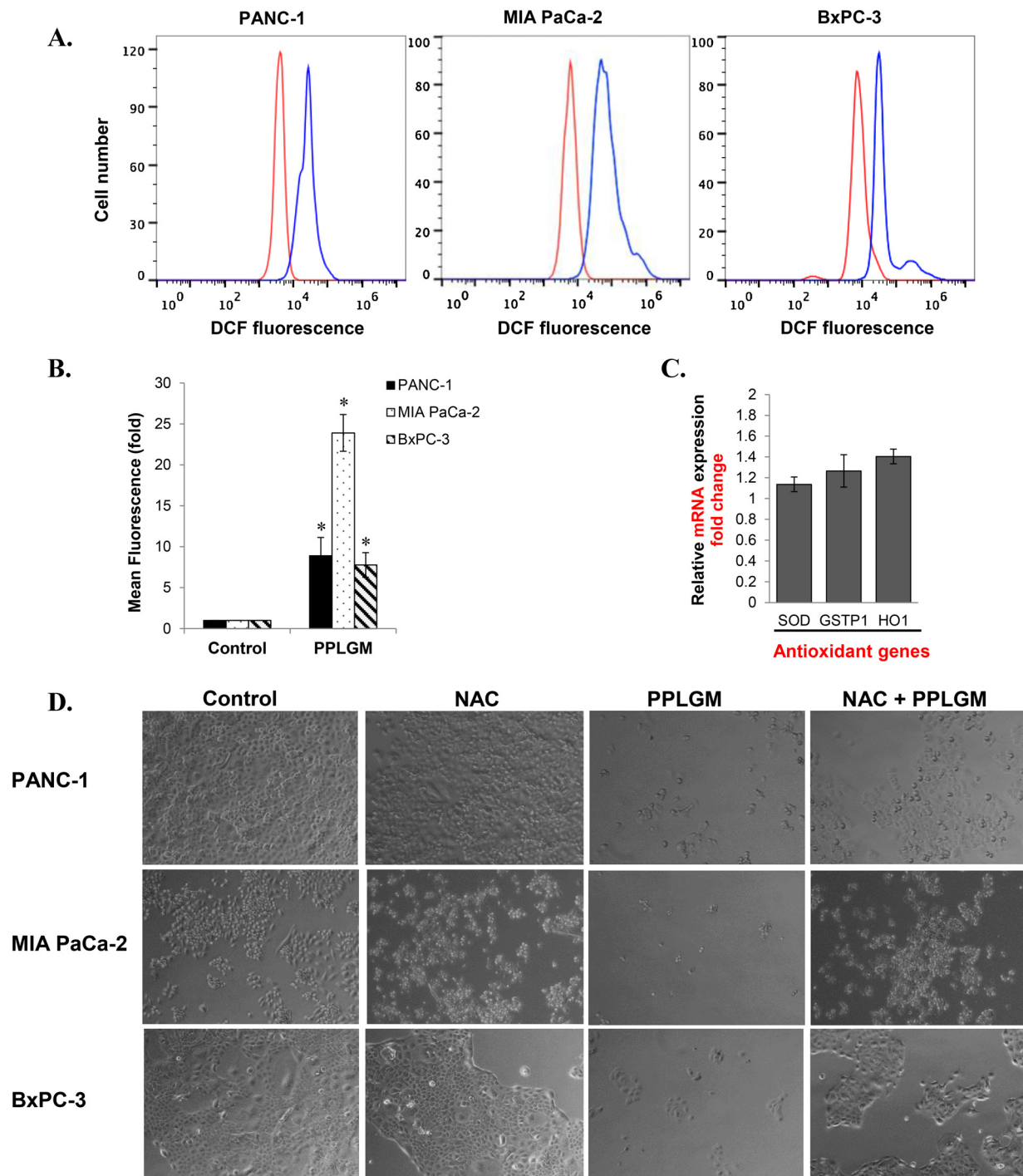


**Fig. 2.** ROS-dependent effects of PPLGM on pancreatic cancer cells. (A) PANC-1, MIA PaCa-2, and BxPC-3 cells were treated with or without 10  $\mu$ M PPLGM for 6 h and analyzed for DCF (an indicator of ROS levels) fluorescence. The red trace shows the fluorescence intensity for DCF in the control-treated cells while the blue trace shows values for the PPLGM-treated cells. (B) The DCF fluorescence intensity obtained in part A was quantified for each PPLGM-treated cell line and related to its respective control and represented as mean fluorescence. (C) PANC-1 cells were treated with 0 or 10  $\mu$ M PPLGM for 24 h and mRNA expression of the antioxidant genes SOD, GSTP-1, and HO-1 was assessed by Q-PCR. 18S rRNA expression in the control and PPLGM-treated cells was used to normalize the data. The mRNA expression fold change for SOD, GSTP-1, and HO-1 are shown for PPLGM-treated cells compared to the control cells. (D) PANC-1, MIA PaCa-2, and BxPC-3 cells were treated with the vehicle (Control), the antioxidant NAC (3 mM), 10  $\mu$ M PPLGM, or 3 mM NAC and 10  $\mu$ M PPLGM for 24 h. The images representing cell survival were taken the next day. The data represent a typical experiment or the average  $\pm$  standard deviation for three independent experiments.

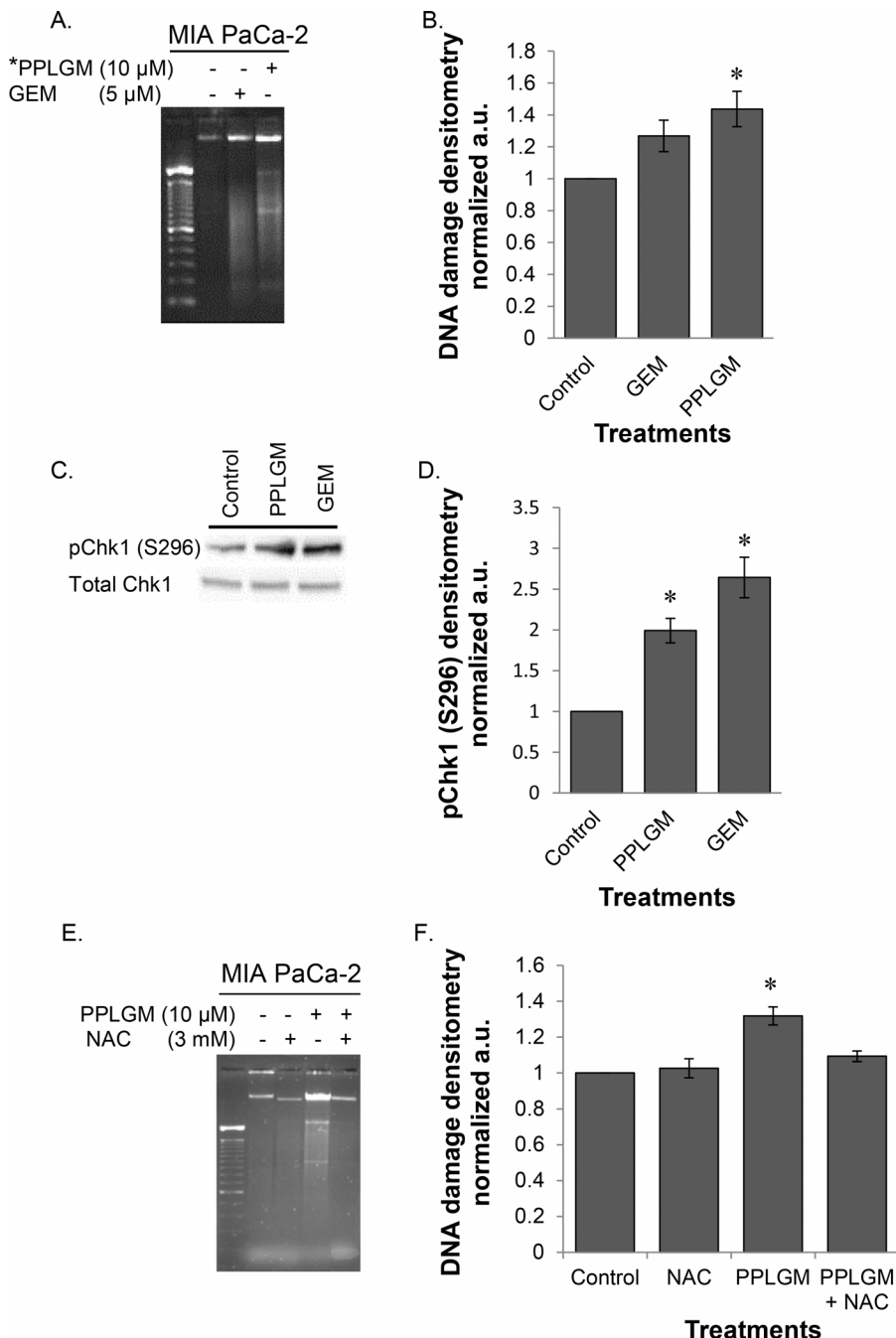


**Fig. 3.** Effect of PPLGM and NAC on DNA damage. (A) MIA PaCa-2 cells were treated for 24 h with 10  $\mu$ M PPLGM or 5  $\mu$ M gemcitabine (GEM) as positive control. The DNA damage was assessed by DNA fragmentation assay on a 1.5% agarose gel and images were captured. (B) Images were quantified using ImageJ software. The intensity of DNA damage in the control lane was compared to the PPLGM and GEM-treated lanes. Densitometry shows the results of PPLGM and GEM treatment on DNA fragmentation normalized to the amount of DNA fragmentation in the control in three replicate experiments  $\pm$  standard deviation. (C) MIA PaCa-2 cells were treated for 24 h with 10  $\mu$ M PPLGM or 5  $\mu$ M GEM as positive control. The cells were lysed to collect protein for western blotting. 60  $\mu$ g protein was loaded into each lane and probed with pChk1 (S296) and total Chk1 antibodies. (D) Quantification of pChk1 (S296) relative to total Chk1 protein was performed by ImageJ software. Densitometry shows the results of PPLGM and GEM treatment on pChk1 (S296) expression normalized to total Chk1 in three replicates  $\pm$  standard deviation. (E) MIA PaCa-2 cells were treated with the vehicle, 10  $\mu$ M PPLGM alone, 3 mM NAC alone, or PPLGM in combination with NAC for 24 h and DNA damage was assessed by DNA fragmentation assay. (F) Densitometry shows the results of PPLGM and NAC treatment on DNA fragmentation normalized to the amount of DNA fragmentation in the control in three replicate experiments  $\pm$  standard deviation where \* denotes statistical significance ( $p < 0.05$ ).

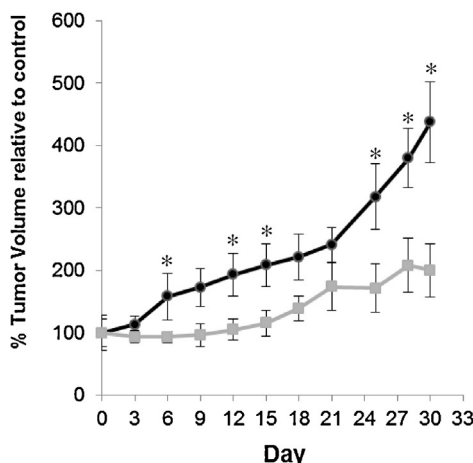


**Fig. 4.** *In vivo* effects of PPLGM in a PANC-1 xenograft mouse model. Intraperitoneal injections of DMSO (1%) and PPLGM (2.4 mg/kg) were administered daily in untreated (●) and PPLGM-treated mice (□), respectively, for 30 days. Subcutaneous PANC-1 tumors were measured every three days. The data represent mean % tumor volume relative to control  $\pm$  standard deviation for 8 animals per group, where \* denotes statistically significant differences ( $p < 0.05$ ).

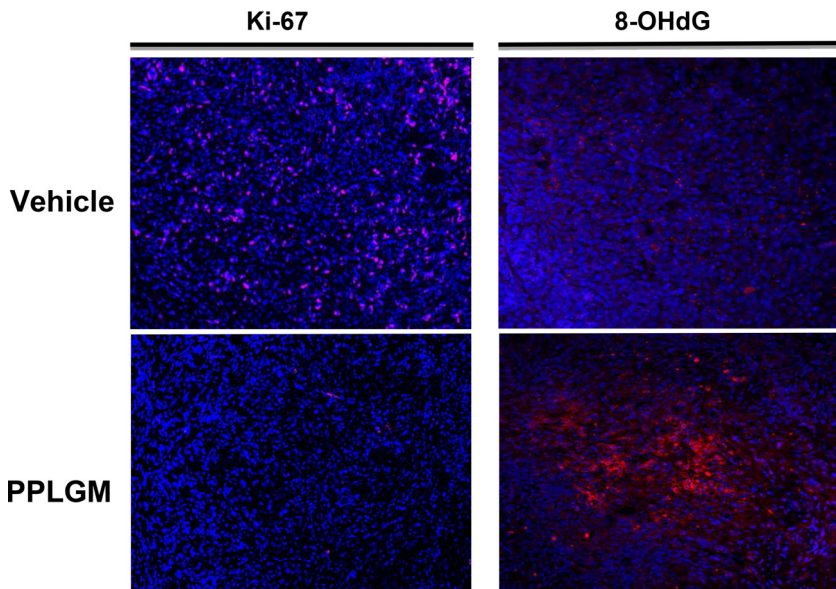


**Fig. 5.** Effects of PPLGM on cell proliferation and the oxidative stress response in PANC-1 xenograft tumors. The tumors were harvested from control and PPLGM-treated animals and were sectioned and stained for Ki-67 (pink) and 8-OHdG (red) expression. DAPI (blue) was used to stain the nuclei. The images show one representative slide for control and PPLGM-treated animals for both Ki-67 and 8-OHdG.

research to pancreatic cancer cell lines harboring wild type *K-ras*. Further, PPLGM interferes with redox homeostasis by elevating ROS levels in all three cell lines without affecting antioxidant enzymes. Additionally, PPLGM causes DNA damage in the MIA PaCa-2 cells. PPLGM-induced DNA damage was reduced in cells treated with an antioxidant NAC, suggesting PPLGM-induced ROS is responsible for DNA damage in these cells. PPLGM also showed anti-cancer effects *in vivo*. For PANC-1 xenografts in nude mice, PPLGM significantly reduced tumor volume compared to the vehicle control. PPLGM-treated tumors displayed elevated levels of an oxidative DNA damage marker (8-OHdG) and reduced expression of a proliferation marker (Ki-67).

**Table 1.** Effect of PPLGM on tumor, organ, and final weight of mice.

	Control	PPLGM
Tumor (mg)	55.9 $\pm$ 19.1	27.7 $\pm$ 4.7
Kidney (mg)	354.3 $\pm$ 13.9	330.8 $\pm$ 11.6
Liver (mg)	1105.9 $\pm$ 24.1	1088.4 $\pm$ 58.0
Lung (mg)	172.6 $\pm$ 8.8	169.5 $\pm$ 5.3
Spleen (mg)	102.4 $\pm$ 12.8	103.7 $\pm$ 7.2
Final Weight (g)	21.8 $\pm$ 1.1	21.7 $\pm$ 0.6

We suggest that ROS-mediated DNA damage plays a role in PPLGM-induced cell death *in vitro* and *in vivo* for pancreatic cancer.

Mutations in the *K-ras* oncogene are detected in the vast majority (>90%) of pancreatic cancers and are thought to play an important role in tumor development, progression, and resistance to chemotherapy and radiotherapy [18]. Cancer patients harboring *K-ras* mutations often have poor prognoses and limited treatment options [19,20]. In this study, we compared the effects of PPLGM on the growth of three different pancreatic cancer cell lines, PANC-1, MIA PaCa-2 and BxPC-3. PANC-1 and MIA PaCa-2 cell lines harbor *K-ras* mutation whereas BxPC-3 cell line contains

wild-type *K-ras*. We found that PPLGM was sensitive to all three cell lines irrespective of the *K-ras* mutation (Fig. 1). This is a promising result since it suggests that PPLGM can be an effective treatment option even for pancreatic cancer patients with oncogenic *K-ras* mutation that are resistant to the currently available therapies.

ROS are constantly generated and eliminated in biological systems, and play an important role in cell signaling pathways [21]. PPLGM has previously been shown to cause enhanced production of hydrogen peroxide and nitric oxide levels in cancer cells but not healthy cells. The anti-cancer effects of PPLGM in cancer cells were attributed to modulation of glutathione S-transferase (GSTP1) activity and glutathione (GSH) levels [13]. However, our study shows that PPLGM elevated ROS levels in all three pancreatic cancer cells without significantly affecting the mRNA expression of three key antioxidant enzymes. Excessive production of ROS can result in many types of DNA damage including single- or double-strand breaks, base modifications, deoxyribose modification, and DNA cross linking. Mild DNA damage can be repaired with or without cell cycle arrest. However, severe DNA damage leads to mutations or induction of cell death or senescence [22]. We found that PPLGM increases DNA laddering and pChk1 (S296) expression in pancreatic cancer cells, and the antioxidant NAC could not only block PPLGM-induced pancreatic cancer death but also offer significant protection against DNA damage. Therefore, ROS-mediated DNA damage is the mechanism for pancreatic cancer cell death but the type of cell death *via* DNA damage needs further investigation.

This study is the first to investigate the anti-tumor efficacy of PPLGM for an animal model of pancreatic cancer. We found that PPLGM (2.4 mg/kg/day for 30 days) significantly inhibited pancreatic tumor growth in the nude mice relative to the vehicle control treatment. The final tumor masses from PPLGM-treated animals were 50% lower than tumors obtained from control-treated animals. Our results are in agreement with previous studies that show intraperitoneal administration of 1.5 mg/kg PPLGM suppresses the growth of bladder, breast, lung and melanoma xenografts by 50–80% nude in mice [13]. However, several mechanisms including oxidative stress can be involved in tumor growth inhibition. Interestingly, the most abundant oxidative DNA lesion produced in response to oxidative stress is 8-hydroxydeoxy guanosine (8-OHDG). Many studies have reported an elevation of 8-OHDG levels in various human cancers and animal models of tumors [23,24]. Our results show that PPLGM markedly increased the levels of 8-OHDG in tumors which may contribute to decreased cell proliferation and tumor growth inhibition.

Taken together, our results demonstrate that PPLGM-induced cell death in human pancreatic cancer cells is mediated by ROS-induced DNA damage. Moreover, PPLGM significantly suppressed the growth of pancreatic tumor xenografts by causing oxidative DNA damage and reduced cell proliferation. Our studies provide a rationale for the development of PPLGM as chemotherapeutic agent against pancreatic cancer in the clinical setting. Further studies evaluating the anti-tumor effects of PPLGM for normal and *K-ras* mutant pancreatic tumors in combination

with chemotherapy are needed to advance this treatment approach to a clinical setting.

## Financial support

NIH/NCRR Grant Number P30 GM103332-01 and the NDSU Development Foundation Centennial Endowment to KMR.

## Conflicts of interest

The authors disclose no potential conflicts of interest.

## Authors' contributions

H. Dhillon and K.M. Reindl conceptualized and designed the study. H. Dhillon, K.M. Reindl developed the methodology. H. Dhillon and S. Chikara acquired the data. H. Dhillon, S. Chikara, and K.M. Reindl analyzed and interpreted the data. H. Dhillon, S. Chikara, and K.M. Reindl wrote, reviewed, and/or revised the manuscript. K.M. Reindl supervised the study.

## Acknowledgements

This publication, and the use of the Core Biology Facility, was made possible by NIH Grant Number P30 GM103332-01 from the National Center for Research Resources. Its contents are solely the responsibility of the authors and do not necessarily represent the official views of the NIH. Additional support was provided by the NDSU Development Foundation Centennial Endowment.

## Appendix A. Supplementary data

Supplementary data associated with this article can be found, in the online version, at [doi:10.1016/j.toxrep.2014.05.011](https://doi.org/10.1016/j.toxrep.2014.05.011).

## References

- [1] R. Siegel, D. Naishadham, A. Jemal, Cancer statistics, CA Cancer J. Clin. 63 (2013) 11–30.
- [2] V. Heinemann, S. Boeck, Perioperative management of pancreatic cancer, Ann. Oncol. 19 (Suppl. 7) (2008) vii273–vii278.
- [3] A. Stathis, M.J. Moore, Advanced pancreatic carcinoma: current treatment and future challenges, Nat. Rev. Clin. Oncol. 7 (2010) 163–172.
- [4] S. Qanungo, M. Das, S. Haldar, A. Basu, Epigallocatechin-3-gallate induces mitochondrial membrane depolarization and caspase-dependent apoptosis in pancreatic cancer cells, Carcinogenesis 26 (2005) 958–967.
- [5] R. Zhang, I. Humphreys, R.P. Sahu, Y. Shi, S.K. Srivastava, In vitro and in vivo induction of apoptosis by capsaicin in pancreatic cancer cells is mediated through ROS generation and mitochondrial death pathway, Apoptosis 13 (2008) 1465–1478.
- [6] I. Jutooru, G. Chadalapaka, P. Lei, S. Safe, Inhibition of NFκappaB and pancreatic cancer cell and tumor growth by curcumin is dependent on specificity protein down-regulation, J. Biol. Chem. 285 (2010) 25332–25344.
- [7] J.P. Fruehauf, F.L. Meyskens Jr., Reactive oxygen species: a breath of life or death? Clin. Cancer Res. 13 (2007) 789–794.
- [8] H. Pelicano, D. Carney, P. Huang, ROS stress in cancer cells and therapeutic implications, Drug Resist. Updat. 7 (2004) 97–110.
- [9] M. Ough, A. Lewis, E.A. Bey, J. Gao, J.M. Ritchie, W. Bornmann, D.A. Boothman, L.W. Oberley, J.J. Cullen, Efficacy of beta-lapachone in pancreatic cancer treatment: exploiting the novel, therapeutic target NQO1, Cancer Biol. Therapy 4 (2005) 95–102.

- [10] L.S. Li, E.A. Bey, Y. Dong, J. Meng, B. Patra, J. Yan, X.J. Xie, R.A. Brekken, C.C. Barnett, W.G. Bornmann, J. Gao, D.A. Boothman, Modulating endogenous NQO1 levels identifies key regulatory mechanisms of action of beta-lapachone for pancreatic cancer therapy, *Clin. Cancer Res.* 17 (2011) 275–285.
- [11] S.J. Cohen, M.M. Zalupska, M.R. Modiano, P. Conkling, Y.Z. Patt, P. Davis, R.T. Dorr, M.L. Boytim, E.M. Hersh, A phase I study of imexon plus gemcitabine as first-line therapy for advanced pancreatic cancer, *Cancer Chemother. Pharmacol.* 66 (2010) 287–294.
- [12] R.T. Dorr, M.A. Raymond, T.H. Landowski, N.O. Roman, S. Fukushima, Induction of apoptosis and cell cycle arrest by imexon in human pancreatic cancer cell lines, *Int. J. Gastrointest. Cancer* 36 (2005) 15–28.
- [13] L. Raj, T. Ide, A.U. Gurkar, M. Foley, M. Schenone, X. Li, N.J. Tolliday, T.R. Golub, S.A. Carr, A.F. Shamji, A.M. Stern, A. Mandinova, S.L. Schreiber, S.W. Lee, Selective killing of cancer cells by a small molecule targeting the stress response to ROS, *Nature* 475 (2011) 231–234.
- [14] H. Randhawa, K. Kibble, H. Zeng, M.P. Moyer, K.M. Reindl, Activation of ERK signaling and induction of colon cancer cell death by piperlongumine, *Toxicol. In Vitro* 27 (2013) 1626–1633.
- [15] M.F. Renschler, The emerging role of reactive oxygen species in cancer therapy, *Eur. J. Cancer* 40 (2004) 1934–1940.
- [16] S. Shankar, G. Suthakar, R.K. Srivastava, Epigallocatechin-3-gallate inhibits cell cycle and induces apoptosis in pancreatic cancer, *Front. Biosci. J. Virtual Library* 12 (2007) 5039–5051.
- [17] R.P. Sahu, S. Batra, S.K. Srivastava, Activation of ATM/Chk1 by curcumin causes cell cycle arrest and apoptosis in human pancreatic cancer cells, *Br. J. Cancer* 100 (2009) 1425–1433.
- [18] S.T. Kim, H. Lim do, K.T. Jang, T. Lim, J. Lee, Y.L. Choi, H.L. Jang, J.H. Yi, K.K. Baek, S.H. Park, Y.S. Park, H.Y. Lim, W.K. Kang, J.O. Park, Impact of KRAS mutations on clinical outcomes in pancreatic cancer patients treated with first-line gemcitabine-based chemotherapy, *Mol. Cancer Ther.* 10 (2011) 1993–1999.
- [19] W. Pao, T.Y. Wang, G.J. Riely, V.A. Miller, Q. Pan, M. Ladanyi, M.F. Zakowski, R.T. Heelan, M.G. Kris, H.E. Varmus, KRAS mutations and primary resistance of lung adenocarcinomas to gefitinib or erlotinib, *PLoS Med.* 2 (2005) e17.
- [20] E. Massarelli, M. Varella-Garcia, X. Tang, A.C. Xavier, N.C. Ozburn, D.D. Liu, B.N. Bekle, R.S. Herbst, I.I. Wistuba, KRAS mutation is an important predictor of resistance to therapy with epidermal growth factor receptor tyrosine kinase inhibitors in non-small-cell lung cancer, *Clin. Cancer Res.* 13 (2007) 2890–2896.
- [21] B.C. Dickinson, C.J. Chang, Chemistry and biology of reactive oxygen species in signaling or stress responses, *Nat. Chem. Biol.* 7 (2011) 504–511.
- [22] O.Z.B. Surova, Various modes of cell death induced by DNA damage, *Oncogene* 32 (2013) 3789–3797.
- [23] R.H. Hsieh, L.M. Lien, S.H. Lin, C.W. Chen, H.J. Cheng, H.H. Cheng, Alleviation of oxidative damage in multiple tissues in rats with streptozotocin-induced diabetes by rice bran oil supplementation, *Ann. N. Y. Acad. Sci.* 1042 (2005) 365–371.
- [24] A. Valavanidis, T. Vlachogianni, C. Fiotakis, 8-Hydroxy-2'-deoxyguanosine (8-OHDG): a critical biomarker of oxidative stress and carcinogenesis, *J. Environ. Sci. Health C: Environ. Carcinogen. Ecotoxicol. Rev.* 27 (2009) 120–139.